UNSYS digital

Journal of Unmanned System Technology

Flow Field of Flapping Albatross-like Wing and Sound Generation at Low Reynolds Number

Sutthiphong Spot Srigrarom

University of Glasgow Singapore
Singapore

***Abstract*—** This paper presents a part of our ongoing development of a bird-like type flapping wing micro-aerial vehicle. Both the unsteady flow and acoustic characteristics of the albatross-like flapping wing were numerically investigated. The flow around the flapping wing was predicted by using ANSYS Fluent unsteady three-dimensional compressible Navier-Stokes equations. The acoustic field was calculated by a built-in acoustic package, based on the FfowcsWilliams-Hawkings (FW-H) acoustic analogy. During the start-up motion, the large start-up vortices dominate the otherwise quiescent field with minimal sound generated. The sound is generated by the rotational and tangential motions of the wing using different sound generation mechanisms. A primary dipole tone at wing beat frequency is generated by the rotational motion, while other dipole tones at higher frequencies are produced by the vortex scattering at the trailing-edge of the wing during the tangential motion. The frequency composition of the primary tone changes with the pitching angle of the wing. During the steady flapping state, the quadruple sound is produced more due to the wake vortex interaction. The far-field sound spectrum is of broader bandwidth. The sound produced propagates only for short distance.

***Keywords*—**Flapping wing, Albatross-like wing, sound generation.

I. INTRODUCTION

There is a growing recognized need for miniature flight vehicles with multifunctional capabilities, such as micro air vehicles (MAVs) for both military and civilian surveillance [1-4]. Flapping wing flight of birds provides us with a sophisticated example of utilizing unsteady aerodynamics to mechanize the miniature flight structures at low Reynolds numbers (10^3-10^5) [5-6]. We attempt to mimic both the long-distance birds, due to their natural long-endurance manner, and their high lift production during take-off (start-up).

The albatross, as shown in **Figures 1a** and **1b**, is chosen to represent long distance migratory birds. It is about the size of our intended flapping wing based surveillance micro-air vehicle (MAV). We hope to mimic albatross's flapping flight to achieve this long-distance characteristic. It is used for investigating flow characteristic aiming at better design of flapping MAV. The wingspan of the albatross is 60 cm. The flapping pattern of the albatross is of the avian type, i.e. vertical motion as shown in **Figure 1c**. Our model simulated the complete, three-dimensional, unsteady flow fields around this type of wing with large-scale vortices.

Corresponding author: Sutthiphong Spot Srigrarom (e-mail: spot.srigrarom@glasgow.ac.uk)

This paper was submitted on July 15, 2013; revised on September 1, 2013; and accepted on September 8, 2013.

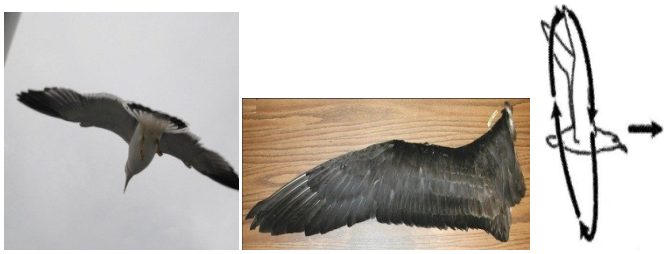

Figure 1 a. Albatross in flight (left), b. Albatross wing model (center), c. The flapping pattern of albatross is avian type, i.e. more up/down vertically

II. COMPUTATIONAL FLUID DYNAMICS CODE

In this paper, we used the commercially available software: ANSYS Fluent® Release 13. The machine that ran these problems was a 64 bit computer, Intel® Core i7-2600 CPU at 3.4 GHz. It had 8 processors, totaling 16 GB RAM. The geometric model of the albatross wing was based on the outline tracing of a royal albatross7. The model wing had a wing span, S of 30 cm, mean wing chord length, c_m of 5 cm, a thickness of 2.5% of the mean wing chord length, as shown in **Figure 1b**. The computing domain extended to 50-chord lengths in all directions around the full model wing, and that, there were about 107 meshes of the tetrahedral type. The flow condition was unsteady transient flow, with the built-in Large-Eddy Simulation (LES) turbulence model. These 10 million meshes appeared sufficient for LES, and were able to capture short wavelengths [8]. To obtain high frequency signals, the time increment was set at $t = 0.001$ s. The flow calculations were 0 to 1 sec physical time. This was sufficient to track the transient static pressure vs. the flow time in order to perform FFT9. The computing time was 5 CPU days.

The wing was originally set at rest. At time $t = 0$, wing was positioned at a 45 degree angle of attack. It started to move (flap) about its z (chordwise) axe, mimicking the start-up of the flapping motion (taking-off). The input angular velocity about its chord (ω_z) is shown in **Figure 2**. This step change refers to sudden pitch-up of the flapping motion (hence, almost infinite start-up torque), which may not truly reflect the actual flapping motion of the albatross, however, the reveals some flow physics, i.e. creation of strong leading edge [10]. From past studies [7,11,12], the starting flapping frequency of the albatross wing was around 0.5 rad/s, corresponding to the reduced frequency k (defined as $c/2U$) of 0.0025. The take-off speed of the albatross (i.e. the freestream velocity in body-fitted coordinates), U was approximately 5 m/s. This gave the Reynolds number, based on chord Re of 25,000.

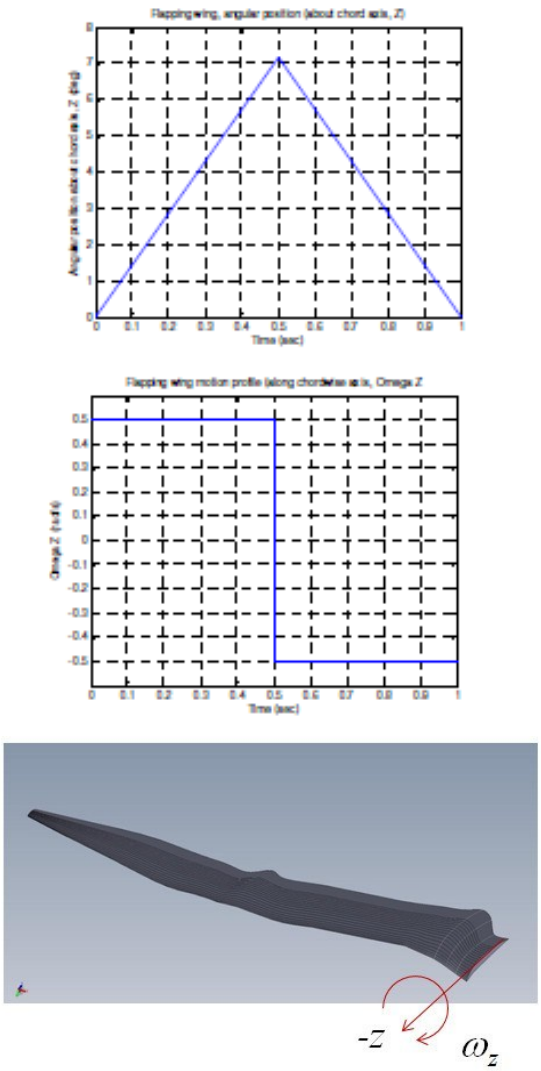

Figure 2 Flapping patterns for albatross about its chord (chordwise, ω_z)

III. Albatross-like Wing Flow Field Results

The results of the albatross flapping motion profile about its wing's chord wise axis (z axis), ω_z are shown in the **Figure 3** (half body). The viewing angle is at a constant position relative to the wing model (body-fitted coordinates). The color of the streamlines shows velocity levels as indicated by the colorbar.

At time t_0 = 0.0 sec, before the flapping motion, the flow around the wing is quiescent, and mostly attached to the wing. There is still wingtip vortex developed at the outer end of the wing. At time t_1 = 0.125 sec, after the flapping motion starts, the wing is set to rotate about its chord, and flaps downwards (away from the reader in both 3D and top views). At the outer half of the wing the flow separated from the wing, forming the start-up vortex which more visible at the top. There is flow separation at the trailing edge, closer to the root, at the area near the scapula (inboard of the wing). Elsewhere, the flow is still attached to the wing. As time goes on (t_2 = 0.25 sec), the flow separates across the wing, forming the strong leading edge vortex over the wing. In the inboard area near the trailing edge and scapula, the wake (shear layers) becomes more obvious. At time, t_3 = 0.375 sec, the start-up vortex becomes bigger, and the flow separates from the wing entirely. At the leading edge near the alula (about half way between the root and the tip), another secondary leading edge vortex structure forms. At time t_4 = 0.5 sec, the start-up vortex breaks away from the wing. The wake at the trailing edge of the wing also breaks up into outer and inner parts.

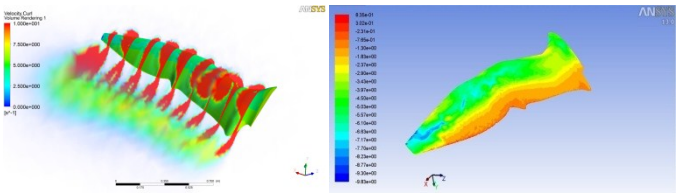

Figure 4 a. Contour of vorticity on the upper part of the Albatross wing, at t_4 = 0.5 sec. The strong leading edge vortex in red color is ob- vious near the wing root. The colorbar indicates the level of vorticity. (left), b. Surface pressure on the albatross wing, at *t4* = 0.5 sec. At the tip, there is region of lower pressure, shown in blue color. (right)

Figure 4a shows the vortices contour at t_4 = 0.5 s, the leading edge vortex is dominant, especially at the inboard part near the root of the wing. Outwards from the root towards the tip, the flow is more attached. At the trailing edge, the wake is generated behind the wing, and so does the noise of primary dipole type. **Figure 4b** shows the surface pressure on the albatross wing also at t_4 = 0.5 sec. At the tip, there is region of lower pressure, shown in blue color. This is the area where the force is less generated. So, we deduce the albatross does maneuvering by flapping its entire left and right wings at different amplitudes than using (flapping or twisting) its wing tip only.

Figure 5 shows the lift and drag coefficients (*CL* and *CD*) on the wing vs. time during flapping motion (**Figure 2**). Together with **Figure 3** and **4**, the leading edge vortex clearly provides significant lift on the albatross wing. The lift increases with the flapping angle.

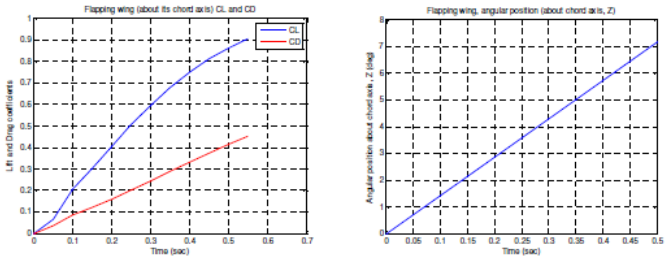

Figure 5 Lift and drag coefficients (C_L and C_D) on the wing (left) versus time during flapping motion, and the wing position (right).

IV. Flapping Wing Noise Calculation

The albatross is known to fly very quietly naturally. The accompanying acoustic signature from their flapping flights is investigated in this section. The calculations for acoustics were done by using the ANSYS Fluent® built-in acoustic package, simultaneously with the unsteady three-dimensional flow calculation using the com- pressible Navier-Stokes equations. The acoustic model used is based on Ffowcs Williams-Hawkings (FW-H) acoustic analogy. According to ANSYS, this FW-H acoustic analogy is the most general

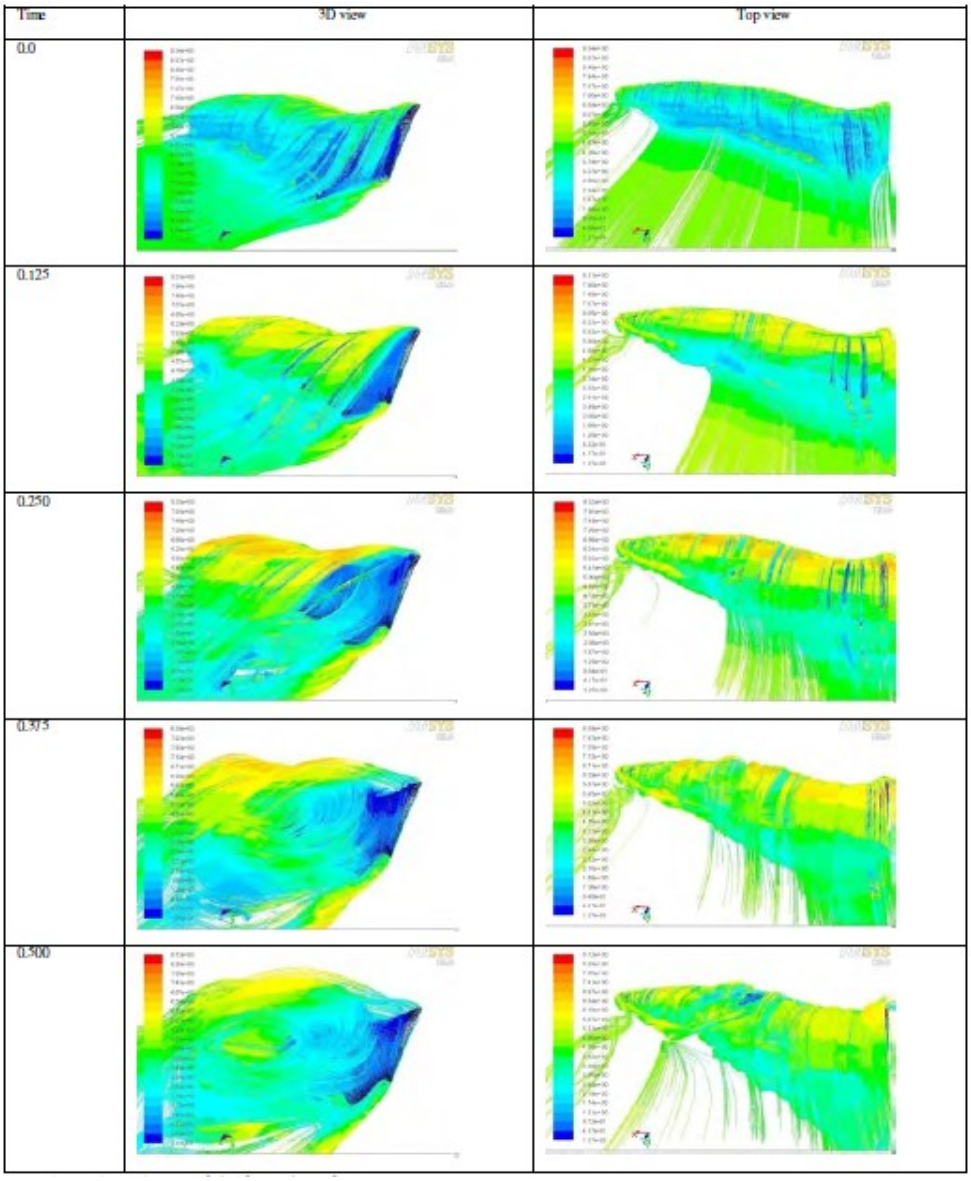

Figure 3 Path lines of the flow about flapping

acoustic integral formulation, valid for moving bodies enclosed by permeable source surfaces, suitable for broadband noise source models [9,13,14].

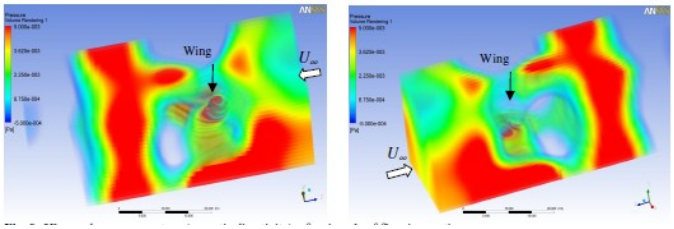

Figure 6 3D sound pressure contour (acoustic directivity), after 1 cycle of flapping motion.

Figure 6 shows the 3D sound pressure contour around the full model wing after 1 flapping cycle (left: horizontally sliced, rear view; right: vertically-sliced, front view). The acoustic directivity can be inferred in this figure. At near field, just behind the wing, the big cavities represent the vortical structure. These large start-up vortices dominate the field. The sound is generated mostly in this near field area, and by the rotational and tangential motions of the wing.

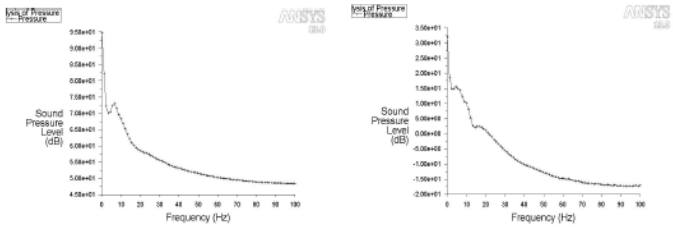

Figure 7 Sound pressure level at different frequencies generated by the wing, after 1 cycle flapping motion, (a) at the wing it- self (left), (b) at 10 chord length behind the wing (right).

Figure 7 shows the sound signatures (distribution of sound pressure in Pascal), at two receivers: one located right at the wing body and another one located far field (10-chord length) behind the wing. At the wing body, the sound level is as high as expected at around 70 dB, with the dominating frequency around 10-20 Hz. The sound is mostly dipole and generated by the flapping motion of the wing. Far downstream, the sound magnitude drops to just about 10 dB, at the same frequency range of 10-20 Hz. Hence, the sound propagates for only a short distance.

V. CONCLUSION

The albatross generates lift on its wing mainly by vortex lift mechanism. We deduce that the albatross does maneuvering by flapping its entire left and right wings at different amplitudes than using (flapping or twisting) its wing tip only. The sound is generated mostly in this near field area, and by the rotational and tangential motions of the wing. A primary dipole tone at wing beat frequency is generated by the rotational (pitching) motion of the wing, and propagates only for short distance.

REFERENCES

[1] DeLaurier, J. D., "The Development of a Full Scale Ornithopter Wing″, *The Aeronautical Journal of the Royal Aeronautical Society*, May 1993.

[2] Ellington, C. P., Van den Berg, C., Willmott, A. P., and Thomas, A. L. R., "Leading-Edge Vortex in Insect Flight," *Nature,* Vol.384, 1996, pp. 626-630. CrossRef

[3] Ellington, C. P., "The Novel Aerodynamics of Insect Flight: Application to Micro- Air-Vehicles", *Journal of Experimental Biology*, Vol. 202, No.23, pp.3439-3448, Dec. 1999.

[4] Gursul, I., and Ho, C. M., "High Aerodynamic Loads on an Airfoil Submerged in an Unsteady Stream", *AIAA Journal,* Vol.30, No.4, 1992, pp. 1117-1120. CrossRef

[5] Liu, H., and Kawachi, K., "A Numerical Study of Insect Flight", *Journal of Computational Physics,* Vol.146, 1998.

[6] Shyy, W., Lian, Y., Viieru D. and Liu H., *Aerodynamics of low Reynolds number flyers*, Cambridge Aerospace Series, ISBN-13: 978- 0521882781, 2008.

Shyy, W., Berg, M, and Ljungqvist, D., "Flapping and Flexible Wings for Biological and Micro Air Vehicles", *Progress in Aerospace Sciences,* Vol. 35, No.5, pp. 455-506, 1999. CrossRef

[7] Doering C. R. & Gibbson J. D., *Applied Analysis of the Navier-Stokes Equation*, Cambridge University Press, 2005.

[8] Fluent Inc, *Advance Acoustics Modelling in Fluent v.6.2*, June 2005, VIEW ITEM

[9] Ol, M., *Unsteady Low Reynolds Number Aerodynamics for Micro Air Vehicles (MAVs)*, US Air Force Research Laboratory , Technical report no. AFRL-RB-WP-TR-2010-3013, May 2010.

[10] Blake, C.H., More data on the wing flapping rates of birds, The Condor, Vol.50, No.4, p.148, 1948. CrossRef

[11] Azuma, A, *The Biokinetics of Flying and Swimming*, AIAA Education Series, 2nd ed, 2006. CrossRef

[12] Howe, M.S., *Acoustics of Fluid-Structure Interactions*, Cambridge University Press, 1998. CrossRef

[13] Bae, Y and Moon, Y.J., "Aerodynamics Sound Generation of Flapping Wing", *Journal of the Acoustical Society of America*, Vol.124, No.1, pp.72-81, 2008. CrossRef